Tellus (1987), *39A*, 72–81

A note on lee wave structures in stratified flow over three-dimensional obstacles

By I. P. CASTRO, *Mechanical Engineering Department, University of Surrey, Guildford, Surrey GU2 5XH, UK*

(Manuscript received January 20; in final form May 6, 1986)

ABSTRACT

An experimental study of the spanwise structure of lee waves generated behind a surface mounted obstacle in linearly stratified flow is described. Attention is concentrated, first, on the conditions under which lee wave breaking always occurs and, second, on the rate at which the wave amplitudes decay across the span. Although only one particular body shape was used—one which promoted boundary layer separation in all cases—it is argued that the form of the results should be generally applicable. The data are compared where possible with the implications of linear theory for a circular hill or a long ridge.

1. Introduction

In a recent experimental study of the stratified flow over triangular ridges of finite spanwise aspect ratio, Castro et al. (1983) (hereafter, CSM) investigated the variation of lee-wave amplitude and slope with aspect ratio and upstream conditions. They presented some photographs of the centre-line (symmetry axis) lee-wave field, some of which clearly showed wave 'breaking'. Whilst many previous workers have also found certain combinations of body geometry and Froude number which led to wave-breaking, both experimentally and theoretically, these have almost always been cases in which the body was two-dimensional. (Froude number is here defined as U/Nh, where U is the upstream velocity, N is the Brunt-Vaisala frequency and h is the obstacle height). For fully 3-dimensional bodies, however, the spanwise extent of the wave-breaking zone must be limited since generally the wave slope decays with spanwise distance from the centre-line. The measurements of CSM were not sufficiently extensive to lead to any definitive conclusions on this point, nor indeed to delineate clearly the 'bounds' which determined when wave-breaking would occur at all. Further, in cases where wave-breaking did not occur, no attempt was made to compare the overall structure of the lee-wave field (apart from the wavelength itself) with the available, though rather limited theoretical work typified by, for example, Crapper (1962) or Lilly and Klemp (1979).

A further series of experiments has been undertaken, with two major objectives in mind. Firstly, to investigate the points mentioned above and, secondly, to study the structure and influence of the upstream propagating columnar modes that can occur in such flows. The latter is a subject of longstanding interest and our results of this aspect of the study, having rather wider implications, are reported separately (Castro and Snyder, 1986; and see also Snyder et al., 1985). In this note we describe only the results of our further investigation of the lee-wave field, with particular reference to the conditions under which wave-breaking will always occur and the spanwise extent and structure of the lee-wave field.

2. Apparatus

All the experiments were conducted in the large towing tank of the EPA Fluid Modeling Facility. Stratification of the nominally 1.1 m deep layer of water was achieved in the usual way by using salt; Thompson and Snyder (1976) contains full details. As in the experiments of CSM, an initially linear density profile with a nominal Brunt-Vaisala frequency of $N = 1.33\ s^{-1}$ was used and the upper few centimeters were syphoned off (with a corresponding layer of brine introduced at the bottom) after every few tows, to maintain the linear profile at the top.

The obstacles used were identical to those of CSM, being of triangular cross-section with flat (vertical) ends. They are clearly somewhat different in shape to most hills or mountains, but the sharp edges have the advantage of fixing the separation lines and therefore avoiding possible complications arising from changes in the latter caused by Reynolds number effects. We wished, in any case, to make comparisons (in the context of the columnar modes) with our earlier work. Some additional similar models were also used to provide a rather wider range of cross-stream aspect ratio. The spanwise aspect ratio, α, is defined as the ratio of the spanwise width of the obstacle (W) to its height (h). Each model was mounted upside down on a baseplate supported by the carriage, and towed at speeds ranging between about 1.2 and 12 cm/s. With a body height, h, of 9 cm and $N = 1.33$, this corresponds to $0.1 < F_h < 1.0$. The baseplate extended upstream and downstream of the obstacles a distance of about $10h$ and $15h$, respectively. It was fitted with a 3 mm diameter boundary layer trip just downstream of the leading edge, and was submerged so that its surface was about 4 mm below the water surface. Fig. 1 shows the general experimental set-up.

Lee-wave fields were visualised by dye streamers injected from a rake of tubes mounted at the leading edge of the baseplate. The flow was illuminated by banks of fluorescent tubes mounted on one side of the tank, and cameras located on the opposite side and underneath were used to obtain permanent records of the flow structure. CSM, Hunt and Snyder (1976) and Thompson and Snyder (1976) give complete details of these experimental arrangements.

3. Results and discussion

3.1. Bounds on lee wave instabilities

At the lower Froude numbers (usually around $F_h = 0.2$) it was not always possible to decide, on the basis of the photographs alone, whether wavebreaking occurred. Fig. 2, for example, shows photographs of the $\alpha = 15$ case; for $F_h = 0.8$ there is evidently a large rotor centred around $z/h = 4$, whereas at $F_h = 0.2$ there does not appear to be any wavebreaking. However, visual observations (of shadowgraph-type) during the tow led to the conclusion that there was, in fact, wavebreaking in this latter case, but it occurred only intermittently during the tow. At these lower F_h values, since wavelengths and amplitudes were much smaller than at higher F_h, breaking sometimes occurred *between* two of the dye streamers without noticeably affecting the streamers themselves. We also noted that occasionally at the higher Froude numbers, wavebreaking, whilst not evident in the photograph, did occur just prior to the end of the tow. Fig. 3 shows photographs of two nominally identical cases, $\alpha = 4$, $F_h = 0.5$. In Fig. 3b breaking has not yet occurred, but the waveslope is evidently critical at around $x/h = 1$, $z/h = 2\frac{1}{2}$ and, in fact, breaking *did* occur just after the photograph was taken. In Fig. 3a, breaking occurred a little earlier in the tow. This was probably because end-wall reflections only became influential late in the tow (Castro and Snyder, 1986).

In Fig. 4, the results of careful observations

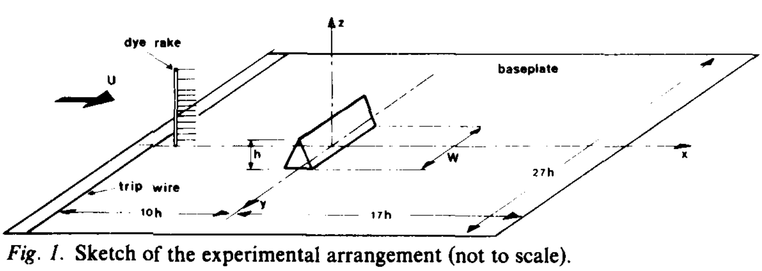

Fig. 1. Sketch of the experimental arrangement (not to scale).

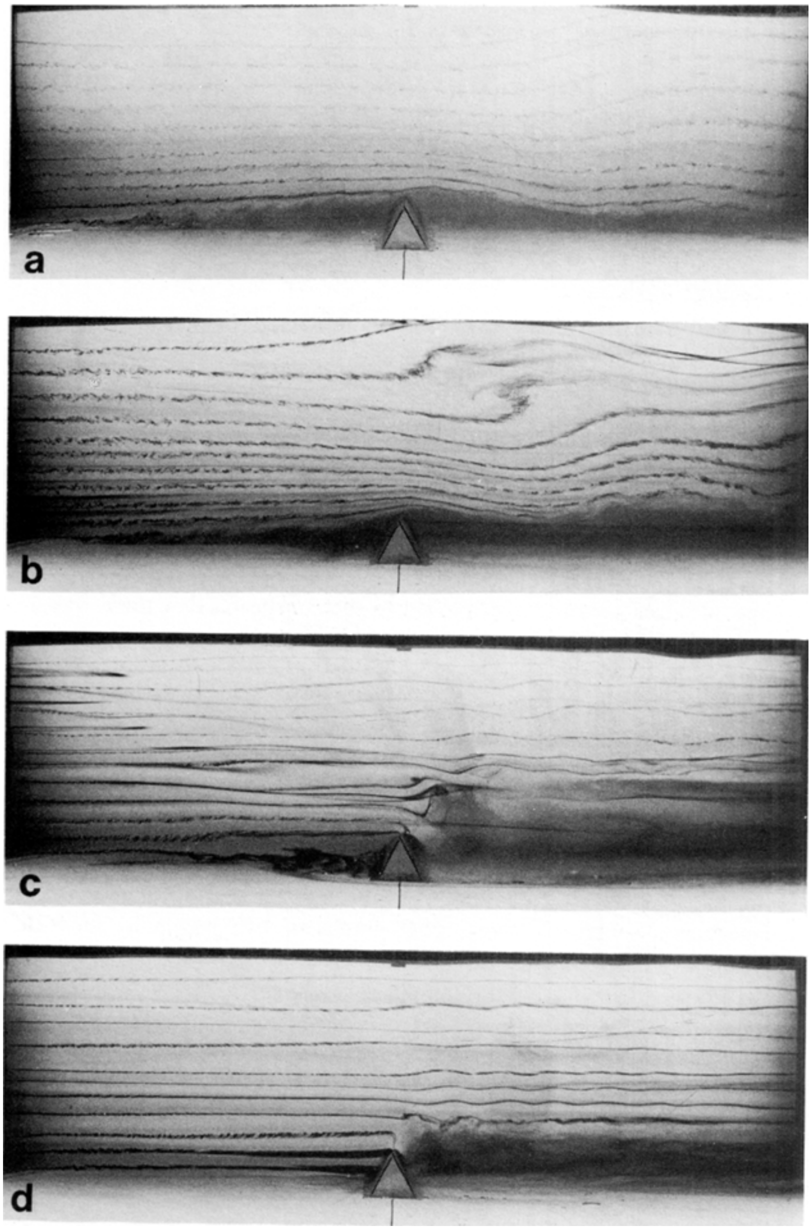

Fig. 2. Dye streamers; $\alpha = 15$. $F_h =$: (a) 0.9; (b) 0.8; (c) 0.3; (d) 0.2.

made throughout each tow are summarised on a F_h/α plot. Each tow made corresponds to one data point and was judged to be either a wave-breaking case or not. Cases like those discussed above, which were near critical, are labelled accordingly and the smooth line represents the 'critical' envelope, within which wavebreaking always occurred and outside of which it never did. (Note that in neutral flow the recirculation region behind the body is of course a direct result of separation from it—there are no wave motions; such regions also occur for $F_h < \infty$ but

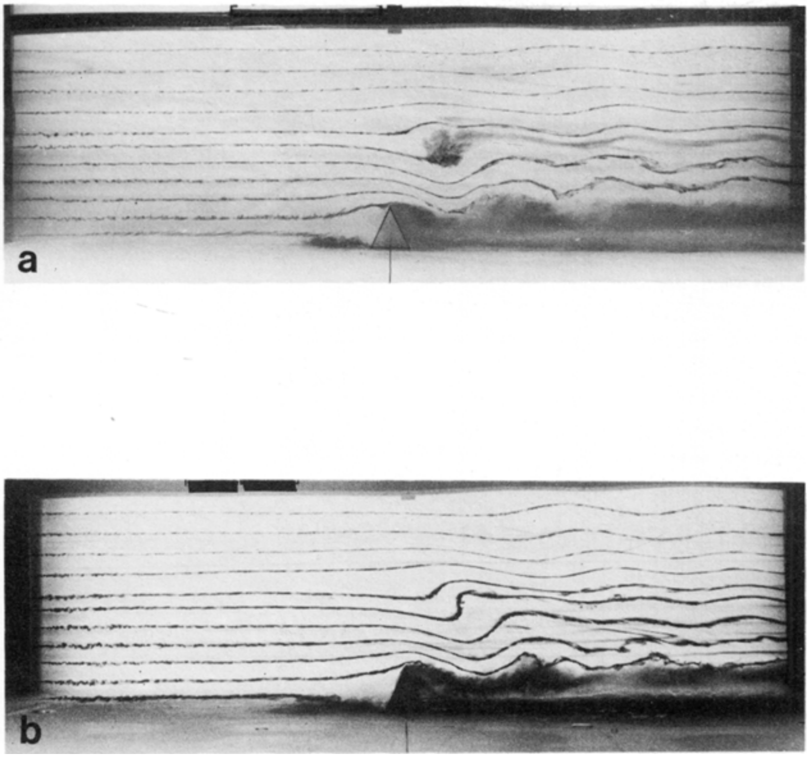

Fig. 3. Dye streamers; $\alpha = 4$, $F_h = 0.5$. Two separate runs.

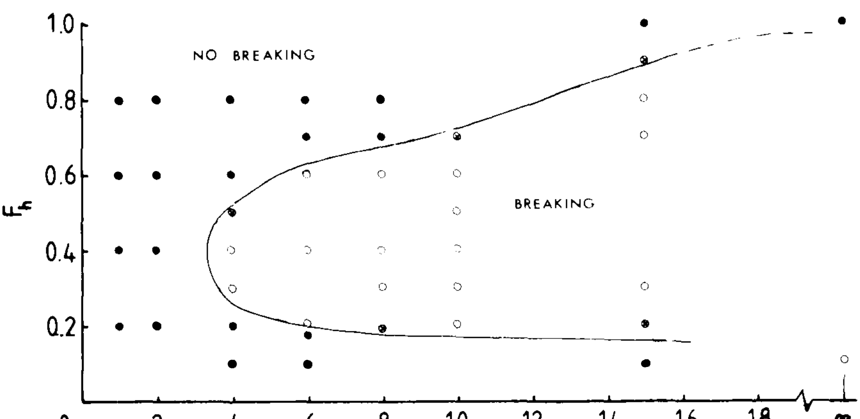

Fig. 4. F_h/α plot showing wavebreaking cases (○) and stable cases (●), with the approximate location of the critical Froude number boundary between them. ⊗ refer to inconclusive tows.

are quite distinct from the rotors that occur as a result of wave breaking). The upper limit on critical Froude number, beyond which rotor formation does not occur, clearly increases slowly with increasing aspect ratio. Now in neutral flow ($F_h = \infty$) an increase in spanwise width of the body is accompanied inevitably by an increase in the length, x_r, of the downstream recirculating region (x_r is measured from the centre of the body to the mean reattachment point on the flow symmetry line, $y = 0$). Variations in wave amplitude for $F_h < \infty$ cannot therefore necessarily be associated solely with an increase in spanwise breadth of the obstacle, for the 'effective' axial length (and shape) may also change. Indeed, CSM showed that although at $F_h = 1.5$, x_r varied much less than for $F_h = \infty$, at $F_h = 0.6$, in contrast, there were significant *non-monotic* variations of x_r with α. At $\alpha = 1$, x_r/h was about 1.5, rising to as much as 10 at $\alpha = 4$ and then falling again to about 2.5 at $\alpha = 8$. However, this non-monotonic variation in x_r with α at fixed F_h is *not* reflected in the incidence of wavebreaking shown in Fig. 4—for $\alpha < 4$ breaking never occurred whereas for $\alpha > 6$ it always did (at $F_h = 0.6$). In other words, the waveslope seems to increase monotonically with α (up to the point at which wave breaking first occurs). This reinforces the conclusion of CSM that the spanwise width of the obstacle is the dominant parameter in determining wave amplitudes (at a given F_h), at least for obstacles which are so steep that separation always occurs.

Some tows were also made of a similar ridge spanning the whole of the tank (with sponge pads sealing the small gaps between its ends and the tank side-walls). There are, of course, serious difficulties in attempting two-dimensional experiments of that sort for $F_h < 1$, as Snyder et al. (1985) have recently demonstrated. Strong upstream columnar modes and flow blocking cause a continual change in the upstream conditions. Furthermore, in a finite length tank, fluid initially lying between the layers at the top and bottom of the obstacle and upstream of it must, as the tow progresses, 'spill' over the top of the obstacle even as $F_h \to 0$, because the total volume of that fluid must be conserved. The lightest layers therefore 'pile up' in front of the obstacle with the heavier layers spilling over behind, so that if the tow ends with the model very near the end wall, the density gradient upstream will be virtually neutral for $z < h$. This is illustrated in Fig. 5 which shows upstream and downstream density profiles after a tow of the $\alpha = \infty$ body at an initial Froude number of 0.2, compared with the initial density profile before the tow. Since the tank is about 25 m long and after the tow the body is within 1 m of the end wall, the

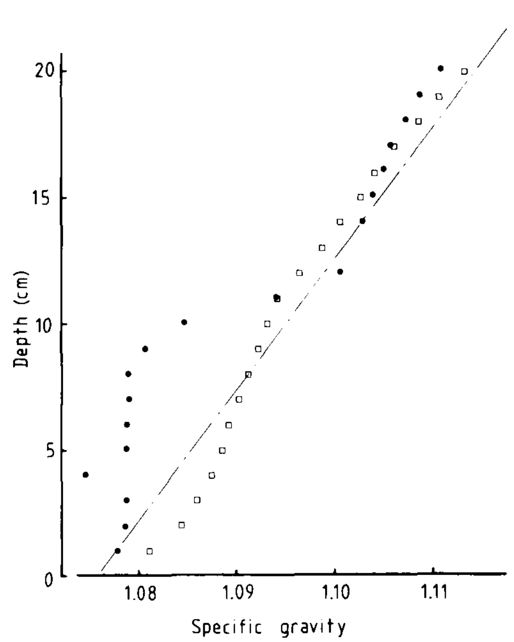

Fig. 5. Density profiles. ------, prior to tow of the $\alpha = \infty$ body at $F_h = 0.2$; □, downsteam and ●, upstream of the body after the tow.

downstream density profile must imply a total mass ($\int \rho dz$) approximately equal to its initial value; the profiles of Fig. 5 clearly satisfy this condition. This 'squashing' phenomenon, along with the usual upstream wave propagation that would occur even without any tank end wall, leads to a continual change of upstream conditions throughout the tow so that a steady-state condition is never reached; Snyder et al. (1985) have provided convincing proof of this, and the problem is discussed more fully in the companion paper to the present one (Castro and Snyder, 1986). However, we found that wave breaking *always* occurred in these 'two-dimensional' runs for $0.1 < F_h < 0.9$, but *never* steadily, unlike all the three-dimensional cases. Often a rotor would appear, then disappear with one, or more, forming elsewhere and this sequence could occur two or three times during the tow. Evidently, the continual change in effective upstream conditions, enhanced perhaps by wave reflections from the end wall, led to continually changing effective Froude numbers. For $F_h = 1.0$, however, wave breaking did *not* occur. We therefore believe that the asymptotic value of the upper critical Froude number (as $\alpha \to \infty$) does not exceed unity.

Lilly and Kemp (1979) have shown that for a two-dimensional bell-shaped mountain with a terrain profile given by $z_h(x) = h/(1 + (x/a)^2)$, overturning first occurs when F_h falls to 1.18. This critical Froude number was shown to increase to about 1.5 for an asymmetric hill of similar downslope but very gradual upslope, and decrease to about 0.5 for the reverse situation. Since the critical Froude number for our two-dimensional triangular ridge is no greater than unity, it appears that the separated wake region causes the obstacle to have, *effectively*, a rather more gradual downslope than the bell shaped mountain.

At the lower end of the Froude number range, wave-breaking never seemed to occur for $F_h = 0.1$ and $\alpha < \infty$. However, the 2-dimensional case did exhibit breaking, which started quite early and remained stable until about half-way through the tow, when the rotor position changed and the flow became unsteady, as described earlier. The asymptotic value of the lower critical Froude number may therefore be somewhat lower than 0.1 but is certainly less than 0.2. It may well depend also on the hill cross-sectional shape (and the upstream velocity profile) but the point is anyway a rather academic one since hills (or buildings) are never 2-dimensional, so that fluid can always 'spill' around the ends, thereby reducing the maximum possible waveslopes and increasing the lower critical Froude number.

3.2. *Spanwise structure of the lee-wave field*

To determine the spanwise extent of the rotor in the wavebreaking cases and the spanwise decay of wave amplitudes in cases where there was no wavebreaking, a number of tows were made with the dye rake positioned off the centreline at various values of y/h. Some typical photographs are presented in Figs. 6 and 7. First, in Fig. 6, the lee-wave fields at $y/h = 0$, 2 and 3 are shown for the $\alpha = 6$, $F_h = 0.4$ case; as Fig. 4 shows, this is a case well inside the critical 'envelope'. $y/h = 3$ corresponds to the end face of the body ($\alpha = W/h = 6$) and it is evident that wave breaking does not extend across the whole span (Fig. 6c). However, it does reach at least $y/h = 2$ (Fig. 6b), so that the rotor is certainly not restricted to around $y/h = 0$ and must, in fact, have a spanwise width in excess of 67% of the obstacle width.

We found that cases nearer, but still within, the critical line in Fig. 4 exhibited wavebreaking over a relatively smaller region. For example, Fig. 6d shows the lee wave pattern for $y/h = 2$ in the $F_h = 0.6$, $\alpha = 6$ case. In this case, the rotor must have a width significantly less than 50% of the body width.

Second, in Fig. 7, the wave patterns at $y/h = 0$, 0.5, 1.0 and 1.5 are shown for $\alpha = 2$, $F_h = 0.6$—a typical case well outside the critical envelope of Fig. 4. The wave amplitudes decrease with increasing y/h and the wave crests and troughs are clearly located somewhat farther downstream as y/h increases. Photographs like those in Figs. 6 and 7 were used to deduce wave slope and the location of peaks and troughs as a function of y/h. Fig. 8 shows the wave slope, measured for the streamer originating at $z/h = 1.6$, plotted against y/W for $\alpha = 2$, 4, and 6, with $F_h = 0.6$. The $\alpha = 6$ case exhibits wave breaking, but the breaking occurs above $z/h = 1.6$, and a wave slope measurement was possible at $y/h = 0$, although the slope was clearly much less than it would have been in the absence of wavebreaking. Similar results could be deduced for streamers originating at different heights—$z/h = 1.6$ was chosen as typical. Fig. 8 implies that the spanwise decay of the waves is relatively more rapid for obstacles that are long in the spanwise direction than for obstacles that are short. However, since there is a separated zone at each end of the obstacle, the 'apparent' width of the body is proportionally greater for smaller bodies. For example, the flow visualisation studies reported in CSM indicated that 'apparent' widths of $6h$ and $11h$ would be more appropriate than the geometric values of $2h$ and $6h$ for the $\alpha = 2$ and 6 cases, respectively. Fig. 9 shows wave amplitudes for three cases plotted against y/W_c, where W_c is a corrected spanwise width, taking into account the size of the separated zones at each end of the body. Within experimental accuracy the data collapse reasonably well, but we have not undertaken a sufficiently extensive survey to be certain that this would always be the case.

Crapper's (1962) linear theory suggests that the spanwise wave decay is more rapid for a circular mountain than it is for long ridge (using

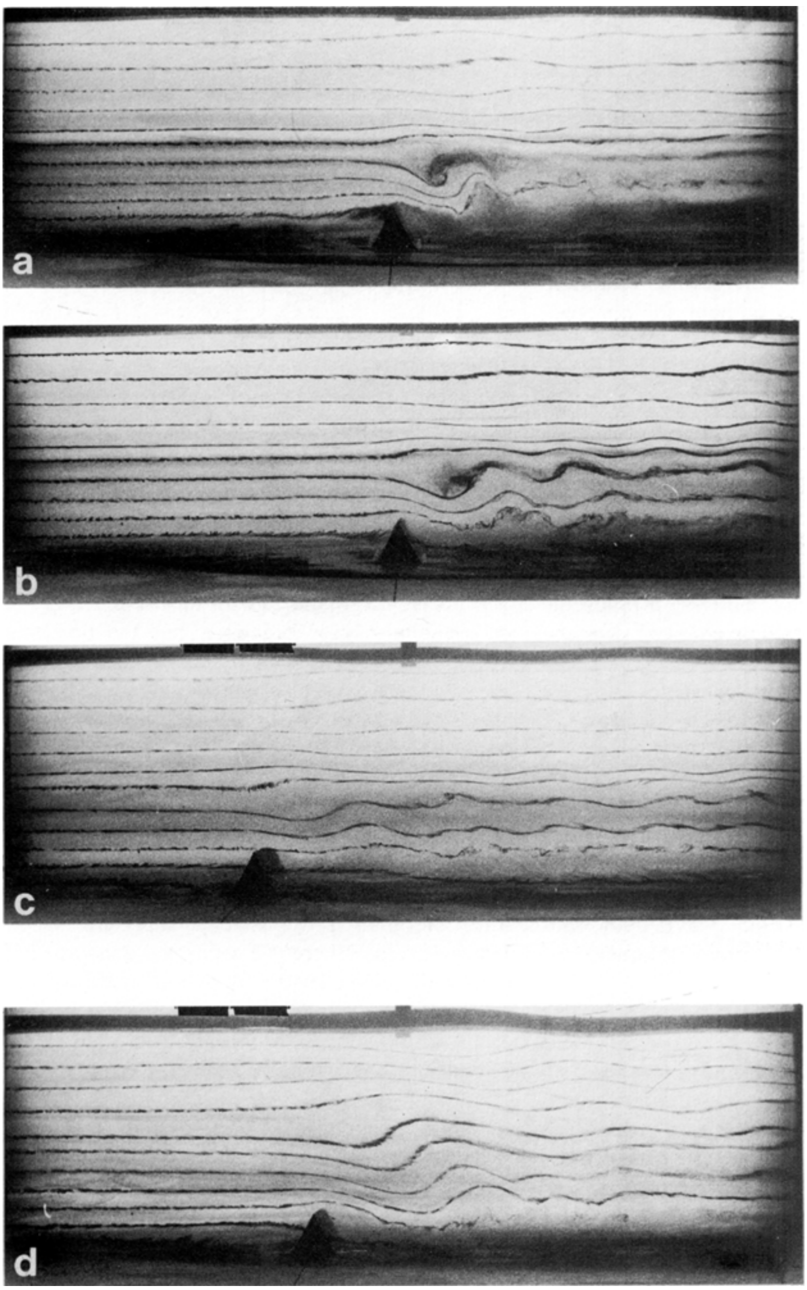

Fig. 6. Dye streamers; $\alpha = 6$, $F_h = 0.4$; $y/h =$: (a) 0; (b) 2; (c) 3; (d) $\alpha = 6$; $F_h = 6$, $y/h = 2$.

$y/$(spanwise width) as the independent variable). Fig. 9 includes the linear theory result for a circular bell-shaped mountain, deduced from Crapper's (1959) results, for a case where F_a (Froude number based on a, the hill radius at $z/h = 0.35$) is about 0.2. This would correspond, perhaps, to the $\alpha = 2$, $F_h = 0.6$ case, for which the separation regions around the obstacle may make

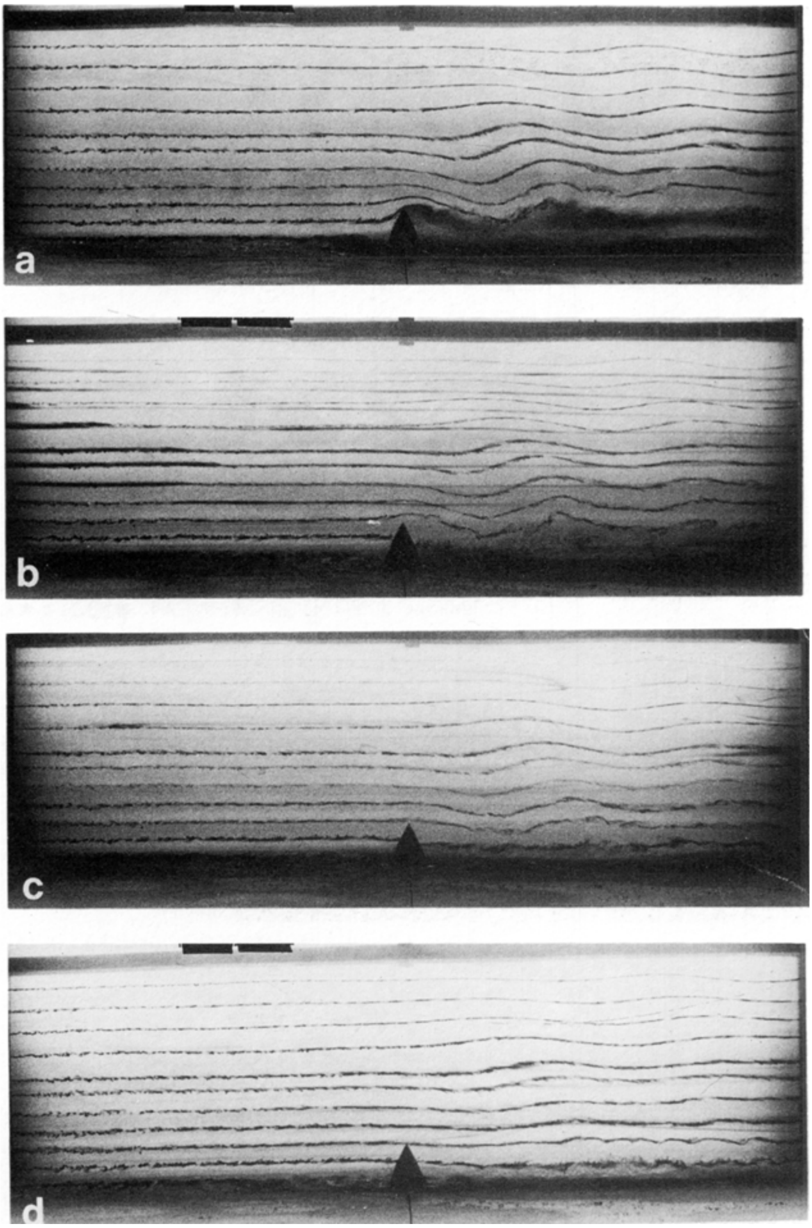

Fig. 7. Dye streamers; $\alpha = 2$, $F_h = 0.6$. $y/h =$: (a) 0; (b) 0.5; (c) 1; (d) 1.5.

it similar, in effect, to a circular hill with $a/h = 3$. The 'long ridge' solution of Crapper (1962) is also included in Fig. 9. Now linear theory suggests that for a long ridge, the decay of wave amplitude with y/W is largely independent of W or F_h, whereas for a circular hill it is not. In that respect the results display a behaviour more like that which linear theory suggests for a long ridge, although the decay is more rapid than that. However, it is not very profitable to attempt detailed comparison with linear theory, since there is no doubt that the perturbations are, in fact, highly non-linear.

Lilly and Klemp's (1979) results suggest that

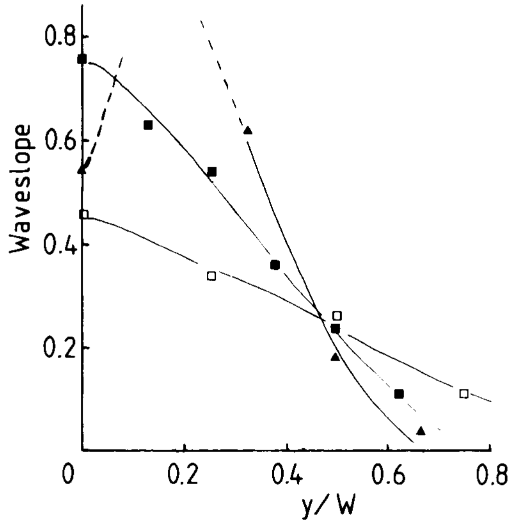

Fig. 8. Waveslope versus y/W for the streamer originating at $z/h = 1.6$. $F_h = 0.6$; $\alpha =$: □, 2; ■, 4; ▲, 6.

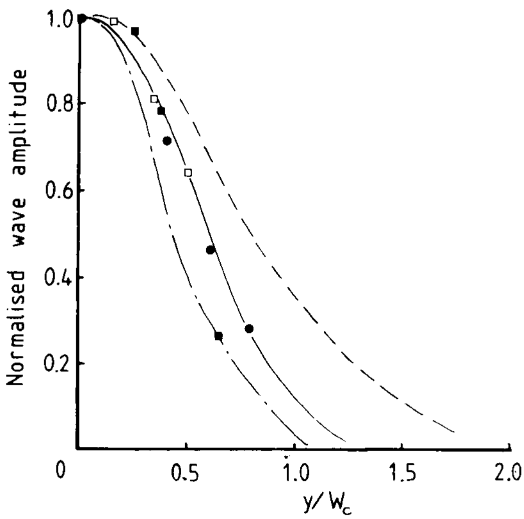

Fig. 9. Wave amplitude normalised by the $y = 0$ values for: □, $\alpha = 2$, $F_h = 0.6$; ■, $\alpha = 4$, $F_h = 0.6$; ●, $\alpha = 6$, $F_h = 0.8$. (Solid line for clarity only). Streamers originate at $z/h = 1.6$ (□, ■) and 2.4 (●). - - - -, linear theory for a long ridge; — — —, linear theory for a circular hill (Crapper, 1959,1962).

non-linear effects change wave amplitudes and slopes (from those expected on the basis of linear theory) much more significantly than phase. Fig. 10 shows the locus of the (first) wave peaks at three different heights for the $\alpha = 4$, $F_h = 0.6$ case. The waves clearly curve downstream as y increases and the curvature is greatest at the lowest heights, as Crapper's (linear) results suggest.

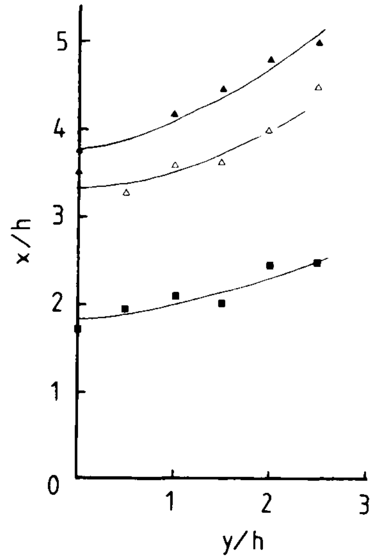

Fig. 10. Locus of the first lee wave crests for streamers originating at $z/h =$: ▲, 1.6; △, 2.4; ■, 3.3. $\alpha = 4$, $F_h = 0.6$.

4. Conclusions

The additional experiments undertaken in this study have been sufficient to, first, determine fairly clearly the conditions under which lee-wave breaking will occur. Fig. 4 is the major result of this aspect of the work. The form of the critical envelope in the F_h/α plot is probably not universal; its position and the asymptotic value of the limiting Froude number (for a 2-dimensional body) above which wave-breaking will not occur, will depend to some extent on the cross-sectional shape of the body and on whether or not separation occurs. As mentioned earlier, overturning behind a two-dimensional bell shaped hill occurs for $F_h < 1.18$ (Lilly and Klemp, 1979); in the present case we did not detect it even at $F_h = 1.0$.

Secondly, the spanwise extent of the wave-breaking, as a proportion of the body width, was found to depend on how close the F_h-α point was to the critical envelope in Fig. 4. For points well within this envelope breaking seemed to occur in a region of width at least 70% of the body span, whereas for points close to the critical line, breaking was more localised near the spanwise centre-line.

Finally, in cases where breaking did not occur, the wave amplitude decayed with distance from the centre-line (normalised by the body span) at a rate that did not depend significantly on either the Froude number or the body aspect ratio, provided the latter was adjusted to account for the size of the separated zones at the spanwise ends. This behaviour is similar to the results of linear theory for a long ridge (Crapper, 1962) although the decay is more rapid than the theory suggests. It is, in fact, rather closer to the linear result for a circular hill (Crapper, 1959). However, since the wave-field in the present experiments was certainly strongly influenced by non-linear effects, really useful comparisons must await the development of non-linear, 3-dimensional theories.

5. Acknowledgements

The author wishes to thank the entire staff of the Fluid Modeling Facility, US Environmental Protection Agency, North Carolina, for their hospitality and technical help at all stages of the work. Particular thanks are extended to his colleague, Dr. W. H. Snyder, for many stimulating discussions. The work was undertaken whilst the author was supported as Visiting Associate Professor, N.C. State University, under Cooperative Agreement No. 807854 with the EPA.

REFERENCES

Castro, L. P., Snyder, W. H. and Marsh, L. 1983. Stratified flow over three-dimensional ridges. *J. Fluid Mech. 135*, 261.

Castro, I. P. and Snyder, W. H. 1986. An experimental study of upstream columnar modes. *J. Fluid. Mech.*, submitted.

Crapper, G. D. 1959. A three-dimensional solution for waves in the lee of mountains. *J. Fluid Mech. 6*, 51.

Crapper, G. D. 1962. Waves in the lee of a mountain with elliptical contours. *Phil. Trans. R. Soc. Lond. A254*, 601.

Hunt, J. C. R. and Snyder, W. S. 1980. Experiments on stably and neutrally stratified flow over a model three-dimensional hill. *J. Fluid Mech. 96*, 671.

Lilly, D. K. and Klemp, J. B. 1979. The effects of terrain shape on non-linear hydrostatic mountain waves. *J. Fluid Mech. 95*, 241.

Snyder, W. H., Thompson, R. S., Eskridge, R. E., Lawson, R. E., Castro, I. P., Lee, J. T., Hunt, J. C. R. and Ogawa, Y. 1985. The structure of strongly stratified flow over hills: dividing streamline concept. *J. Fluid Mech. 152*, 249.

Thompson, R. S. and Snyder, W. H. 1976. EPA fluid modeling facility. In Proc. Conf. on Modeling and Simulation, Envir. Prot. Agcy Rep., EPA-600/9-76-016, Wash. D.C., July.